# Correlations Between Analyses and Forecasts of Banded Heavy Snow Ingredients and Observed Snowfall

Michael Evans and Michael L. Jurewicz Sr.

National Oceanic and Atmospheric Administration / National Weather Service Forecast Office

Binghamton, New York

Submitted November 20, 2007

Corresponding Author: Michael S. Evans, National Weather Service Forecast Office, 32 Dawes Drive,

Johnson City, NY 13790

Michael.Evans@noaa.gov

## Abstract

North American Mesoscale (NAM) model forecasts of the occurrence, magnitude, depth, and persistence of ingredients previously shown to be useful in the diagnosis of banded and/or heavy snowfall potential are examined for a broad range of 25 snow events, with event total snowfall ranging from 10 cm (4 inches) to over 75 cm (30 inches). The ingredients examined are frontogenetical forcing, weak moist symmetric stability, saturation, and microphysical characteristics favorable for the production of dendritic snow crystals. It is shown that these ingredients, previously identified as being critical indicators for heavy and/or banded snowfall in major storms, are often found in smaller snowfall events. It is also shown that the magnitude, depth, and persistence of these ingredients, or combinations of these ingredients, appear to be good predictors of event total snowfall potential. In addition, a relationship is demonstrated between temporal trends associated with one of the ingredients (saturated, geostrophic equivalent potential vorticity) and event total snowfall.

Correlations between forecast values of these ingredients and observed snowfall are shown to decrease substantially as forecast lead time increases beyond 12 hours. It is hypothesized that model forecast positioning and timing errors are primarily responsible for the lower correlations associated with longer-lead forecasts. This finding implies that the best forecasts beyond 12 hours may be produced by examining diagnostics of heavy snow ingredients from a single, high-resolution model to determine snowfall potential, then using ensemble forecasting approaches to determine the most probable location and timing of any heavy snow.

Formatted: Right: -72 pt

## 1. Introduction

Numerous theoretical and observational studies have shown that bands of heavy snow often occur in regions where upward vertical motion associated with forcing for large-scale ascent is enhanced within the ascending branch of a thermally direct circulation associated with strong, steeply sloped lower to midtropospheric frontogenesis Snowfall within these regions can be particularly heavy when the enhanced upward motion becomes co-located with a region of reduced or negative stability to slantwise motions, within a saturated environment (e.g., Bennetts and Hoskins 1979; Martin 1998a, b; Nicosia and Grumm 1999; Schultz and Schumacher 1999). Based on these studies, forecasters engaged in predicting snowfall have been trained to look for favorable configurations of large-scale forcing, frontogenesis, reduced or negative moist symmetric stability, [as indicated by small or negative values of saturation geostrophic equivalent potential vorticity (EPVg<sup>\*</sup>)], and high relative humidity. A favorable configuration for heavy snow organized in bands features a region of reduced or negative EPVg\*, co-located with high relative humidity, and located above and on the warm side of a region of frontogenesis (Fig.1). In addition, ascent maximized within a layer where temperatures are near -15°C favors the production of dendritic snow crystals (Rogers and Yau 1989), which can improve precipitation efficiency (Auer and White 1982). Thus large-scale forcing, frontogenetical forcing, weak moist symmetric stability, saturation, and microphysical characteristics favorable for the production of dendritic snow crystals are considered as ingredients for heavy snowfall, consistent with previous ingredients-based methodologies (e.g., Wetzel and Martin 2001).

While much research and forecaster training during the past several years has focused on applying these concepts to major snowstorms, a growing body of case study research indicates that events associated with lighter snowfalls also feature many of the same signatures commonly associated with heavier snow events (e.g., Banacos 2003; Schumacher 2003; Jurewicz and Evans 2004; Evans 2006, Novak et al. 2006, Wagner

2006). The implication of this finding is that some of the conceptual models that have been applied to forecasting heavy snow can also be applied to forecasting lighter snowfall events. However, these findings also imply that merely identifying the existence of frontogenesis, weak moist symmetric stability, sufficient moisture and a favorable lift and temperature profile may be insufficient to discriminate between heavy and lighter snow events. Wagner (2006) examined four cases featuring moderate snowfall amounts; and hypothesized that the intensity, depth, and persistence of these ingredients may be important to determining event total snowfall for a given storm.

The purpose of this study is to test the hypothesis that event total snowfall for a storm is correlated not only to the existence of certain key ingredients associated with conceptual models for banded and/or heavy snowfall, but also to the intensity, depth, and persistence of these ingredients. The ingredients examined in this study will be ingredients related to mesoscale forcing, stability and microphysics. The hypothesis will be tested by examining a large number of snow events characterized by a wide range of snow accumulations. In addition, this study will examine how reliable model forecasts of these ingredients are at short ranges, and how rapidly that accuracy degrades with increasing lead time.

Section 2 of this paper will present the study methodology. Section 3a will show correlations between event total snowfall and model analyses through 6 h forecasts of the magnitude, depth, and persistence of frontogenesis forcing, stability, vertical motion, moisture, and temperature. Section 3b will show the same correlations, except for 12 and 24 h forecasts. Section 3c introduces some figures developed for forecasters based on the results of the study. Some examples are shown in section 4, and the paper concludes with a discussion in section 5, and a summary in section 6.

## 2. Methodology

Snow events that affected the Binghamton, New York (BGM) National Weather Service (NWS) Weather Forecast Office (WFO) county warning area (CWA) during the period from 2003 through 2006

were examined. The BGM CWA includes the region from central New York through northeast Pennsylvania. In order to be included in the study, the snow event had to contain a period when reflectivity of at least 30 dBZ was observed on the BGM Weather Surveillance Radar - 88 Doppler (WSR-88D) (Klazura and Imy, 1993). A representative "event maximum snowfall" was determined for each event, by examining radar reflectivity at 6-hourly (00, 06, 12 and 18 UTC) intervals, and identifying the time and location where a snow band, clearly not associated with lake effect snow (e.g. Niziol et al. 1995), appeared to be most intense based on reflectivity data. The event maximum snowfall was the maximum observed snowfall that occurred in the vicinity of the band, based on reports from spotters and NWS cooperative observers within the BGM CWA, with obvious outliers excluded. This methodology occasionally had the desired effect of excluding locations with higher snowfall totals that occurred away from the primary snow band, and were likely inflated at least in part by lake effect snow occurring at the end of the event. To give the study a better representation in the major storm category, three additional cases were included where extremely heavy snow fell just outside the BGM CWA. Finally, events were excluded if the location that received the event maximum snowfall also received a significant amount of liquid or freezing precipitation. The date of each storm event, event-maximum snowfall, and the location of the event maximum snowfall, is given in Table 1.

For each event, data from the North American Mesoscale (NAM) model, run operationally at the National Center for Environmental Prediction (NCEP) approximately 0-24 h prior to the time of heaviest snowfall, was collected. The NAM was run with a grid spacing of 12 km and 60 vertical levels during this period (Rogers et al. 2001). NAM data was archived on the CONUS 212 grid (a 40 km, Lambert Conformal grid covering much of North America), with 3 h temporal, and 25 hPa vertical resolution up to 500 hPa, and 50 hPa vertical resolution above 500 hPa. For events where the minima or maxima of a particular element occurred between the three hourly time steps, the values were muted, but are still considered representative

relative to other events. A 40 km grid was chosen, since 80 km data would not resolve many of the mesoscale features that were being studied, whereas tight gradients associated with 12 km data might cause features to be missed when examining data at single points. The data was examined on NWS Advanced Weather Information Processing System (AWIPS) workstations.

To examine depth and persistence of key features, time-height diagrams were calculated for each event at a point near the event maximum snowfall. "Analysis" time-height diagrams were created by examining data from successive 0-6 h forecasts, initialized during the period when the majority of the snow fell at the point. Time-height data were also obtained from "12 h" forecasts, defined as forecasts from a single NAM run, initialized approximately 12 h prior to the heaviest snow (as determined by radar animations), at the point. Finally, "24 h" forecasts were obtained from a single NAM run, initialized approximately 24 h prior to the heaviest snow, at the point. The primary advantage of examining data in time-height format is that the persistence of key features can be analyzed, along with their depth and magnitude. However, the disadvantage of examining data in this way is that some features may be missed, if the point is not placed in a representative location, especially in areas where tight gradients exist.

Data were also viewed using conventional cross sections to mitigate problems associated with collecting data from time-height displays. Cross sections were oriented normal to the 1000-500 hPa thickness gradients, at times and locations when and where the snow was most intense (based on radar reflectivity), and 3-6 hours prior to when the snowfall was most intense. The conventional cross sectional data were obtained from NAM model forecasts, initialized at times zero to six hours prior to the most intense snowfall. Data were collected at locations along the cross section that were 50 km or less from the center of the most intense observed radar reflectivity associated with snow. The primary advantage of examining data in cross sectional format is that the entire width of the snow area was sampled, mitigating the risk of missing important features when examining data at a single point. However, this approach gives

less information on the persistence of key features than the time-height method. Thus, the time-height and cross-sectional analyses provide complementary approaches.

To examine NAM forecasts of the magnitude, depth, and persistence of frontogenetical forcing, Fn vector convergence was calculated (Keyser et al. 1988). Fn is defined in natural coordinates as:

$$\mathbf{F}\mathbf{n} = |\nabla \theta| \cdot [\partial \mathbf{v}_n / \partial \mathbf{n}] \tag{1},$$

where  $\theta$  is the potential temperature,  $\nabla$  is a two-dimensional gradient ("del") operator, n is the direction parallel to  $\nabla \theta$ , and v<sub>n</sub> is the two-dimensional component of the full wind in the n direction. Fn vector convergence is proportional to the forcing for vertical motion due to full-wind, 2-D frontogenesis. A visual inspection of the data on the 40 km grid indicated that values of Fn convergence > 5 x10<sup>-14</sup>°C s<sup>2</sup> m<sup>-1</sup> were often associated with substantial upward vertical motion. Therefore, depth and persistence of Fn convergence > 5 x10<sup>-14</sup>°C s<sup>2</sup> m<sup>-1</sup> was examined as a proxy for depth and persistence of substantial frontogenetical forcing. Since the conceptual model for banded snowfall discussed in the introduction indicates that the causative frontal-scale forcing should occur primarily in the mid-troposphere, and since the primary goal of this study is to test the conceptual model for a wide range of snow events, Fn convergence maximum values were only calculated between 900 hPa and 400 hPa (shallow, surface-based forcing was disregarded).

Saturated, geostrophic equivalent potential vorticity (EPVg\*) was calculated to examine NAM forecasts of the magnitude, depth, and persistence of moist symmetric stability:

 $EPVg^* = -\zeta_g \cdot \nabla \theta_{es}$ (2),

where  $\zeta_{g}$  is the three-dimensional geostrophic vorticity vector and  $\theta_{es}$  is the saturation equivalent potential temperature.

 $EPVg^*$  is negative in areas of conditional instability, inertial instability, or conditional symmetric instability (CSI) (Schultz and Schumacher 1999). Therefore, the depth and persistence of  $EPVg^* < 0$  PVU, co-located with relative humidity greater than 80 percent, was examined as a proxy for depth and persistence of moist symmetric instability in a near-saturated environment. Since the conceptual model being tested in this study refers to instability located above frontal-scale forcing,  $EPVg^*$  was only calculated between 850 and 400 hPa (shallow layers of surface-based instability were disregarded).

In order to look for *combinations* of favorable conditions for enhanced snowfall, a \* Signature was defined as any area on a cross section or time-height diagram where omega was  $< -8 \ \mu b \ s^{-1}$  (omega < 0 indicates upward vertical motion), EPVg\* was negative, and relative humidity was greater than 80%. Unlike EPVg\* and Fn convergence, minima of omega were obtained by sampling the entire column. Likewise, a \*\* Signature was defined as any area on a cross section or time-height diagram where omega was  $< -12 \ \mu b \ s^{-1}$ , EPVg\* was negative, and relative humidity was greater than 80%. Omega  $< -8 \ \mu b \ s^{-1}$  was invariably associated with at least some frontogenetical forcing, therefore the \* and \*\* Signatures were identifying regions where frontogenetical forcing, instability, and sufficient moisture (the three main ingredients for banded, heavy snowfall) were all present. Finally, a "dendrite signature" was defined as any area on a cross section or time-height diagram where omega was  $< -8 \ \mu b \ s^{-1}$ , in combination with a temperature between  $-12^{\circ}$  and  $-18^{\circ}$ C, and relative humidity > 80%. The decision to use  $-8\mu b \ s^{-1}$  and  $-12\mu b \ s^{-1}$  as thresholds for "moderate" and "strong" upward vertical motion was largely dependent on the choice to examine data on 40 km grids. Smaller grid spacing would have required higher threshold values, and larger grid spacing would have required lower thresholds.

The depth and persistence of selected parameters were quantified by plotting the parameters' values on

the time-height diagrams described earlier, on an AWIPS workstation. Each plot was converted into an electronic image and opened into the GNU Image Manipulation Program (GIMP) (www.gimp.org/about/). The feature of interest was manually outlined, and the number of pixels within the outline was calculated by the GIMP software. A large number of pixels would indicate a deep, and / or persistent feature, while a small number of pixels would indicate that the feature was less deep, and / or persistent. (The vertical axes on the time-height diagrams were logarithm of pressure, which insured that pressure decreased at a nearly constant rate with increasing height on the diagram through the lower and mid-troposphere). The number of pixels was then divided by the number of pixels comprising a standardized area on the time height diagram, represented by an area that was 15 h long and 700 hPa deep. The result was a standardized percent value, which correlated to the depth, and or persistence of the feature in question.

Once this procedure was executed for each parameter and event in the study, a database was constructed that contained the following for each event: observed event maximum snowfall, event maximum magnitude of each parameter (from analysis, 12 and 24 h forecast time-height diagrams), a standardized percent value representing the depth and persistence of each parameter (from analysis, 12 and 24 h forecast time-height diagrams), and a maximum value of each parameter within 50 km of the most intense snowfall, during, three h prior to, and six h prior to the most intense snowfall (from conventional cross sections). Correlations were calculated between the observed event maximum snowfall and the other parameters in the database. Since the data was not normally distributed [the majority of snowfall events ranged from 10 to 30 cm (4 to 12 inches), with a diminishing number at higher values], the correlations were calculated using the Spearman coefficient of rank correlation (Gibbons, 1976).

## 3. Results

#### a. Correlations derived from NAM analyses

Conventional cross sections, at the time of maximum snowfall intensity, showed that negative EPVg\* was found in 22 out of 25 storms in the study, somewhere in the layer between 850 and 400 hPa, within 50 km of the most intense snowfall. Meanwhile, values of Fn convergence  $> 5 \times 10^{-140}$ C s<sup>2</sup> m<sup>-1</sup> were found in all 25 events, a \* Signature was found in 19 out of 25 cases, and a \*\* Signature was found in 13 of 25 cases. Finally, a dendrite signature was found in 16 of the 25 cases. These results indicate that the primary ingredients for major snowstorms also occurred with many of the weaker storms in this study.

The analysis data obtained from the time-height diagrams showed that 24 of the 25 events included a forecast of at least some negative EPVg\*, somewhere in the layer between 850 hPa and 400 hPa, at some time during the period of snowfall. Meanwhile, 22 of the 25 events featured Fn convergence values of at least 5  $\times 10^{-14}$ °C s<sup>2</sup> m<sup>-1</sup>, somewhere in the layer between 900 and 400 hPa, 20 of the 25 events were associated with a \* Signature, and 16 of 25 events were associated with a \*\* Signature. Finally, 21 of the 25 events contained a forecast of omega < -8µbs<sup>-1</sup> in the dendrite zone, at some time during the period of snowfall. These results indicate that merely identifying the existence of the ingredients is insufficient for determining event total snowfall. It can be hypothesized, however, that the magnitude, depth, and persistence of the ingredients may be critical for determining event total snowfall.

Correlations between event maximum snowfall and maximum / minimum values of the aforementioned ingredients, based on data derived from the conventional cross sections, are summarized in Table 2. Statistically significant (at a 0.95 percent confidence level) correlations were found between event maximum snowfall and minimum omega in the dendrite zone (0.63), minimum omega (0.35) and maximum Fn convergence (0.54). The correlation between observed snowfall and the minimum value of EPVg\*, within 50 km of the heaviest snow along the cross-sectional axis, was not significant (0.32). However,

significant correlations were found between event maximum snowfall and both the depth and minimum value of negative EPVg\*, 3 h prior to the time of the heaviest snowfall (0.48 and 0.58, respectively). This finding implies that minima in EPVg\* were occurring in these model analyses just prior to the onset of the heaviest snowfall, during the more significant events.

Table 3 shows correlations between event maximum snowfall, and the maximum/ minimum values of the aforementioned ingredients, based on data derived from the time-height diagrams. In general, the correlations between maximum snowfall and event maximum / minimum values of the ingredients at a single point (Table 3) appeared to be lower than correlations between maximum snowfall and maximum / minimum values of the ingredients sampled in cross sections during the time of heaviest snowfall (Table 2). In particular, the minimum value of omega had a very low correlation with snowfall (0.18). An exception was the minimum value of EPVg\*, which exhibited a robust correlation of 0.63.

The correlations between observed snowfall and the model analysis *depth and persistence* of the ingredients in this study (from time-height diagrams) are summarized in Table 4. Parameters are listed in order from highest to lowest correlation with event maximum snowfall. In general, parameters associated with depth and persistence of the ingredients exhibited larger correlations with event maximum snowfall than parameters associated with event maximum / minimum values. The depth and persistence of omega < - 8  $\mu$ b s<sup>-1</sup> in the dendrite zone showed the highest correlation with event maximum snowfall (0.70), followed closely by the depth and persistence of the \* Signature (0.61) and omega < -8  $\mu$ b s<sup>-1</sup> (0.59). The depth and persistence of negative EPVg\* and Fn vector convergence > 5 x10<sup>-14</sup> c s<sup>2</sup> m<sup>-1</sup> also correlated significantly with event maximum snowfall (0.56 and 0.34, respectively). Perhaps surprisingly, the lowest correlation with event maximum snowfall was found with the \*\* Signature (0.17). This may be an indication that the model analysis and short-term forecasts were less reliable when it came to properly placing and timing areas of intense lift associated with \*\* Signatures (omega < -12  $\mu$ b s<sup>-1</sup>), than in properly placing and timing the

broader areas of less intense lift associated with the \* Signature (omega < -8  $\mu$ b s<sup>-1</sup>).

## b. Correlations derived from 12 and 24 h NAM forecasts

Correlations between event maximum snowfall and the magnitude, depth, and persistence of several ingredients derived from 12 h and 24 h NAM forecasts are shown in Figs. 2 and 3, respectively. Some of the correlations between event maximum snowfall and the magnitude, depth, and persistence of the parameters in the study increased between 0 h and 12 h, while others decreased. All of the correlations decreased between 12 h and 24 h. The correlations associated with the magnitude, depth and persistence of ingredients not including omega (ie EPVg\* and Fn convergence) are all below the 0.95 significance threshold of 0.35 at 24 h. Meanwhile, most of the correlations associated with parameters that include omega (ie omega, omega in the dendrite zone, and the \* Signature), appear to degrade more slowly. The exception is the \*\* Signature, which exhibited a correlation of 0.10 at 24 h, indicating that the NAM was quite poor at properly timing and placing intense areas of lift associated with the \*\* Signature at that time range.

#### c. Forecast applications

The above correlations highlight that identifying the magnitude, depth and persistence of several key parameters is critical to forecasting event-total snow amounts. To highlight these results, the data has been organized into graphs designed to aid with forecasting event-total snowfall amounts. Some examples of these graphs are shown in Figs. 4 and 5. Figure 4a indicates that the vast majority of events in the study with total snowfall over 20 cm (8 inches) were associated with \* Signatures. However, the data also indicates that the majority of events with total snowfall less than 20 cm were also associated with \*

Signatures. Thus, the fact that the \* Signature usually occurs, regardless of snowfall total (at least for storms with maximum snowfall totals of greater than 10 cm (4 inches)), means that the \* Signature is not a good discriminator between heavy and lighter snowfall events. (However, the lack of a \* Signature can be used to rule out the possibility of a 34+ cm (14+ inch) storm).

A potentially more useful approach to discriminate between heavy and lighter snowfall events is to consider the depth and persistence of a \* Signature. Specifically, the data in Fig. 4b indicates that events associated with a maximum snowfall of greater than or equal to 35 cm (14 inches) were always associated with \* Signatures at least 50 hPa deep, that persist for at least 3 hours. By contrast, events of less than 20 cm were not typically associated with this "deep, persistent" \* Signature. Results for events between 20 and 35 cm were inconclusive. These results imply that heavy snowfall events can be discriminated from light events by looking for the existence of a deep, persistent \* Signature.

The benefits of examining values of upward vertical motion within the dendrite zone, as opposed to examining upward vertical motion without regard to the thermal profile, can be seen by examining the data in Figs. 5a and 5b. Figure 5a shows data from conventional cross sections, at the time and location of peak snow band intensity. Event total snowfall is plotted against minimum omega in the dendrite zone. The results show a good delineation between "lighter" snowfall cases and more significant ones, based on the magnitude of the dendrite zone omega. In Fig. 5b, also using data from conventional cross sections, at the time and location of peak snow band intensity, event total snowfall was plotted against minimum omega in the column, without regard to the thermal or moisture profiles. In contrast to Fig. 5a, there was a much wider variation in the magnitudes of the minimum omega, particularly for the lower snowfall events. These results indicate that the main value of assessing sustained ascent in the dendrite zone is that this parameter is effective at separating cases with lower snowfall from cases with larger snowfall, even when other parameters may look more favorable. To further illustrate this point, using comparisons to event maximum

snowfall, there was a noticeably higher correlation to the strongest omega within the dendrite zone (0.63), versus the strongest omega without regard to thermal and moisture profiles (0.35, Table 2). Waldstreicher (2001) found similar results regarding the relationship between thermal profile and snow amounts, when he examined a large collection of storms over central New York.

#### 4. Examples

Examples of NAM forecasts of the ingredients discussed in this paper are shown in Figs. 6 and 7, to illustrate some of the key points in this paper. Figures 6a-d show an example of how details in the NAM forecast can be unreliable at 24 h lead times. The data on Fig. 6a shows a time-height diagram from a forecast for a winter storm made at a point in eastern New York that received around 60 cm (24 in) of snow. The heaviest snowfall at the point fell around 06-12 UTC on the 6<sup>th</sup>, or about 18 to 24 hours after this forecast was initialized. The forecast indicated a minimum of omega just under 8  $\mu$ bs<sup>-1</sup>, co-located with negative EPVg\* (indicated by the grey shading) and relative humidity greater than 80 percent for about 3 h around 00 UTC on the 6<sup>th</sup>, indicating a short-lived, shallow \* Signature, and no \*\* Signature. The data shown in Fig. 6b is valid at the same point and time as the data in Fig. 6a, but is derived from the NAM model run 18 h after the forecast shown in Fig. 6a. In contrast to Fig. 6a, pronounced \* and \*\* Signatures are indicated by a prolonged period of omega < - $12 \,\mu bs^{-1}$ , co-located with negative EPVg\* and near saturated conditions. Figures 6c and d show plan view displays of forecast omega and negative EPVg\*, both valid at 06 UTC on the 6<sup>th</sup>. Figure 6c shows 18 h forecast data from the 12 UTC, December 5 run of the NAM, and indicates a weak band of upward vertical motion at 600 hPa extending from Pennsylvania northeast across central New England. Negative EPVg\* at 500 hPa, indicated by the grey shading, does not appear to be colocated with the upward vertical motion over eastern New York. The same data from the 06 UTC,

December 6<sup>th</sup> run of the NAM (Fig. 6d) shows a much stronger band of upward vertical motion over the area of interest, co-located with a much larger area of negative EPVg\*.

Figures 7a-d show examples from an event where temporal trends of elevated instability may have played an important role in band development and intensity. Figures 7a and 7b show vertical cross-sections of EPVg\* (shaded) and relative humidity (black contours) valid at 06 UTC and 09 UTC respectively on 16 April, 2007. Band intensity and associated snowfall rates reached their peak from about 09-12 UTC across central New York State (Fig. 7d), with snowfall totals ultimately exceeding 50 cm (20 inches) over this region. Approximately 3 h before the snow band reached its peak intensity for this case, negative EPVg\* spiked in both magnitude and depth (Figs. 7b and c). By 09 UTC, the column had stabilized considerably, with negative EPVg\* no longer evident in an area coincident with the main snow band (Figs. 7b and c).

## 5. Discussion

This study examined 25 snow events with maximum snowfall accumulations ranging from 10 cm (4 inches) to over 75 cm (30 inches), and found that frontogenesis, weak moist symmetric stability, sufficient moisture, and significant upward vertical motion in the dendrite production zone could be identified in the majority of cases, regardless of event total snowfall. Thus, meteorologists engaged in forecasting snowfall amounts need to focus on additional factors that provide better discrimination between large and small events. Wagner (2006) hypothesized that identifying the magnitude, depth, and persistence of these ingredients could yield insight on the snowfall potential of an upcoming storm. The main purpose of this study was to test this hypothesis.

Statistically significant correlations were found between event total snowfall and 00 to 6 h forecasts of

the magnitude, depth and persistence of frontogenetical forcing and negative EPVg\* (Tables 2, 3 and 4). Since EPVg\* < 0 was only identified in near saturated regions, this parameter was also related to depth and of saturation, and thus all three of the ingredients for heavy, banded snowfall identified in Novak et al. (2006) were examined and found to correlate significantly with observed snowfall. In an attempt to leverage the utility of examining combinations of all three of these ingredients, the \* Signature was defined to identify instances when strong upward vertical motion (invariably associated with significant frontal-scale forcing) was juxtaposed with moist symmetric instability and saturation. As indicated in Fig. 4a, it was found that a \* Signature almost always appeared in heavier snow events, but also frequently occurred with lighter events, yielding a potentially high false alarm ratio for anyone trying to use the existence of the \* Signature to forecast heavy snow. However, if the depth and persistence of the \* Signatures are taken into account, results improved (Fig. 4b), allowing more light events to be eliminated from consideration as potentially heavy snow producers. An important point regarding the usage of the \* Signature, as including omega < -8  $\mu$ b s<sup>-1</sup>, would not be valid for higher or lower-resolution data.

Correlations between event maximum snowfall and the forecast magnitude, depth, and persistence of the ingredients in this study decreased with increasing lead time beyond 12 h. This finding has several important implications for forecasters. For example, the low correlations at 24 h do not necessarily indicate that these ingredients should not be examined at that time range. Indeed, examination of the magnitude and depth of these ingredients on plan view and conventional cross-sectional displays, 24 h or more prior to the occurrence of heavy snow would likely still give forecasters valuable information on the snowfall potential of an impending storm. However, the low correlations of these ingredients displayed on fixed-point time-height diagrams indicate the high potential for forecast positioning and timing errors at longer time ranges. These errors indicate that forecasters should not rely too heavily on individual model solutions for

forecasting details on placement and timing of heavy snow bands at 24 h forecast time ranges. A more effective approach may be to combine output from an ensemble forecast system, in order to ascertain the most likely location of significant features, with output from a single, high-resolution model, to gain insight on the snowfall potential of the event (e.g., Roebber et al. 2004; Novak and Colle 2007). In general, our results imply that 12 km NAM forecasts of magnitude, depth, persistence, and location of key heavy snow ingredients, displayed on a 40 km grid, can be used with reasonably high confidence at time ranges of 12 h or less, consistent with the forecast strategy of Novak et al. (2006). Beyond 12 h, confidence in the details of these forecasts decreases, particularly regarding placement and timing of key features. These results indicate that the examination of forecasts of these ingredients on plots with grid spacing of 40 km or less (as opposed to 80 km) at extended forecast ranges is a questionable practice, given that the high level of detail shown at this resolution may not only make these plots noisy and difficult to interpret, but may also be unreliable.

Despite the high correlations between depth and persistence of the \* Signature and event maximum snowfall, this study was unable to demonstrate that these correlations were significantly higher than correlations between event maximum snowfall and depth and persistence of omega  $< -8 \ \mu b \ s^{-1}$  (Table 4). However, "snap-shot" values of the depth and magnitude of some of the ingredients did have higher correlations to total snowfall than "snap shot" values of the magnitude of maximum upward vertical motion (based on conventional cross sections, taken across the width of the band, near times and locations of peak intensity). Specifically, parameters with significantly higher correlations to event maximum snowfall than the minimum value of omega (0.35; Table 2) included: 1) the magnitude of maximum Fn vector convergence (0.54; Table 2), 2) the magnitude and depth of EPVg\* three hours prior to the most intense banding (0.58 and 0.48; Table 2), and 3) the magnitude of omega in the dendrite zone (0.63; Table 2). These findings may indicate that the real value of diagnosing ingredients, or combinations of ingredients

(other than just omega), is at the approximate time and location of when and where the snow will be most intense.

The finding that EPVg\* tends to minimize prior to band development in major storms, with a decrease in negative EPVg\* during band maturity, was also observed by Novak et al. (2008) in a case study of the 25 December 2002 northeast U.S. snowstorm. This finding implies that the NAM may be realistically simulating the release of instability during snow band formation and intensification. This hypothesis provides an interesting analogy to warm season convective processes, when stability indices (both from model-derived proximity soundings and observed soundings) often indicate a maximum in convective instability prior to thunderstorm development. The operational implication of this finding is that forecasters should insure that they assess stability in a potential snow-banding environment both during and *just prior to* the period of expected snow band maturity.

Most of the lighter snowfall events in the database had relatively low magnitudes of upward vertical motion within the dendrite zone, near the time and location of peak snow band intensity. Also, if vertical motion was evaluated in the column without regard to the associated thermal profile, the magnitude of upward vertical motion for the lighter snowfall cases showed significant variability. Thus, it appears that the technique of looking for favorable crystal growth mechanisms (strong upward vertical motion in the dendrite zone) may allow forecasters to eliminate some events for consideration as heavy snow producers, thereby lowering false alarm ratios. These results substantiate earlier work by Waldstreicher (2001), who also showed that looking for lift juxtaposed with a favorable thermal profile could help discriminate between large and small events.

## 6. Summary

The results from this study indicate that the primary ingredients previously identified as critical components of heavy snow events also occur in weaker storms. The results also indicate that identifying the magnitude, depth, and persistence of these ingredients should be a key component of the forecast process when trying to determine event total snowfall. Finally, the results from this study demonstrate that the reliability of NAM forecasts of these ingredients, at a point, decreases substantially with increasing forecast lead-time beyond 12 h. These results indicate that high-resolution diagnostics of ingredients at longer time ranges are of limited value to forecasters, as the details of these forecasts will likely contain timing and placement errors. As such, we recommend that forecasters restrict examination of high-resolution (12-40 km) diagnostics to forecast ranges of 12 hours or less. Beyond 12 h, lower-resolution (80 km) diagnostics of ingredients can be examined to give forecasters a general idea of storm potential. Forecasters can augment these diagnostics with ensemble prediction systems to assess the highest probabilities of when and where the potential will be realized.

## 7. Future Work

This paper focused on correlations between observed snowfall and ingredients previously identified as being critical for the development of heavy, banded snowfall. One factor that was not correlated to observed snowfall in this study was NAM quantitative precipitation forecasts (QPFs). QPFs were not included, since the focus of this study was on ingredients, and model QPF, while certainly a key indicator of snowfall potential for operational forecasters, cannot strictly be considered an ingredient (as defined by Wetzel et al. 2001). In addition, it was determined that a rigorous evaluation of model QPF for the cases in our study was beyond the scope of this research. However, it can be

hypothesized that model QPF should correlate strongly to the ingredients shown in this paper, particularly omega. As such, strong correlations likely exist between model QPF and observed snowfall. The key question that still needs to be answered is whether or not operational utilization of the ingredients in this study can allow forecasters to improve on model QPFs. To answer this question, a thorough evaluation of model QPFs would need to be done for the cases in this study, along with calculations of corresponding correlations between observed snowfall and model QPF. Proof of the hypothesis that examination of model ingredients can help forecasters improve on model QPF would require finding significant correlations between certain characteristics of the ingredients (such as magnitude, depth or persistence) and the quality of the model QPF.

Another area of study that was not undertaken by this project would be to employ a similar methodology to examine the relationship between observed snowfall and characteristics of large-scale forcing, along with characteristics of the juxtaposition between large-scale and mesoscale forcing. For example, Schumacher (2003) has suggested that diagnosing the relative positioning of large-scale and frontal-scale forcing may be a critical step in snowfall forecasting.

*Acknowledgments.* The authors would like to thank Dan Keyser and Lance Bosart from SUNY Albany for their helpful comments during the research phase of this project. We would also like to thank Ron Murphy, ITO at BGM, for his help with collecting the data for the study, and Justin Arnott at BGM for reviewing the manuscript. We would also like to thank David Novak at NWS Eastern Region Headquarters Scientific Services Division for providing many helpful comments during the project, and a review of this manuscript. Finally, we would like to thank the work of 3 anonymous reviewers who made many helpful comments during the final phase of the project.

- Auer, A. H., Jr. and J.M. White, 1982: The combined role of kinematics, thermodynamics and cloud physics associated with heavy snowfall episodes, J. Meteor. Soc. Japan, 60, 591-597.
- Banacos, P. C., 2003: Short range prediction of banded precipitation associated with deformation and frontogenetical forcing, Preprints, 10<sup>th</sup> Conf. on Mesoscale Processes, Portland, OR, Amer. Meteor. Soc., CD-ROM, P1.7.
- Bennetts, D. A., and B.J. Hoskins, 1979: Conditional symmetric instability-a possible explanation of frontal rain bands. *Quart. J. Roy. Meteor. Soc.*, **105**, 945-962.
- Doswell C. A. III, H. E. Brooks, and R. A. Maddox, 1996: Flash flood forecasting: An ingredientsbased methodology. *Wea. Forecasting*, **11**, 560–581.
- Evans, M. S., 2006: An analysis of a frontogenetically forced early-spring snowstorm. Bull. Amer. Meteor. Soc., 87, 27-32.
- Gibbons, J. D., 1976: Nonparametric methods for quantitative analysis. American Sciences Press Inc., copyright by Holt, Rinehart and Winston, 463pp.
- Keyser, D., M. J. Reeder, and R. J. Reed, 1988: A generalization of Petterssen's frontogenesis function and its relation to the forcing of vertical motion. *Mon. Wea. Rev.*, **116**, 762-781.

- Jurewicz, M. L., and M. S. Evans, 2004: A comparison of two banded, heavy snowstorms with very different synoptic settings. *Wea. Forecasting*, **19**, 1011-1028.
- Klazura, G. E., and D. A. Imy, 1993: A description of the initial set of analysis products available from the NEXRAD WSR-88D system, *Bull. Amer. Meteor.*, **74**, 1293-1311.
- Martin, J. E., 1998a: The structure and evolution of a continental winter cyclone. Part I: Frontal structure and the occlusion process. *Mon. Wea. Rev.*, **126**, 303-328.

\_\_\_\_\_, 1998b: The structure and evolution of a continental winter cyclone. Part II: frontal forcing of an extreme snow event. *Mon. Wea. Rev.*, **126**, 329-348.

- Nicosia, D. J., and R. H. Grumm, 1999: Mesoscale band formation in three major northeastern United States snowstorms. *Wea. Forecasting.*, 14, 346-368.
- Niziol, T.A., W.R. Snyder and J.S. Waldstreicher, 1995: Winter weather forecasting throughout the eastern United States. Part IV: Lake effect snow. *Wea. Forecasting.*, **10**, 61-77.
- Novak, D. R., J. S. Waldstreicher, D. Keyser, L. F. Bosart, 2006: A forecast strategy for anticipating cold season mesoscale band formation within eastern U.S. cyclones. *Wea. Forecasting.* **21**, 3-23.

, and B. A. Colle, 2007: Assessing the predictability of band formation and evolution during three recent northeast U.S. snowstorms. *Preprints, 22<sup>nd</sup> Conf. on Weather Analysis and Forecasting*, Park City, UT, Amer. Meteor. Soc., P1.29A.

- , Colle, B. A., and S. E. Yuter, 2008: A high resolution observational and modeling study of an intense mesoscale snowband over the northeast U.S. *Mon. Wea. Rev.*, **136**, 1433-1456.
- \_\_\_\_\_\_, B. A. Colle, and S. E. Yuter, 2007: A high-resolution observational and modeling comparison of mesoscale band life cycle during three recent northeast U.S. snowstorms. *Preprints, 22<sup>nd</sup> Conf. on Weather Analysis and Forecasting*, Park City, UT, Amer. Meteor. Soc., 3A.2
- Roebber, P. J., D. M. Schultz, B. A. Colle, and D. J. Stensrud, 2004: Toward improved prediction: high-resolution and ensemble modeling systems in operations. *Wea. Forecasting*, **19**, 936-949.
- Rogers, R.R., and M.K. Yau, 1989: A Short Course in Cloud Physics. Pergammon Press, New York, 293 pp.

- Rogers, E., T. Black, B. Ferrier, Y. Lin, D. Parrish, and G. DiMego, 2001: Changes to the NCEP Meso Eta Analysis and Forecast System: Increase in resolution, new cloud microphysics, modified precipitation assimilation, modified 3DVAR analysis.
  NOAA/NWS Technical Procedures Bulletin 488, 21 pp. [Available online at <a href="http://www.emc.ncep.noaa.gov/mmb/mmbpll/eta12tpb/">http://www.emc.ncep.noaa.gov/mmb/mmbpll/eta12tpb/</a>; also available from Office of Climate, Water, and Weather Services, National Weather Service, 1325 East–West Highway, Silver Spring, MD 20910.].
- Schultz, D. M., and P. N. Schumacher, 1999: The use and misuse of conditional symmetric instability. *Mon. Wea. Rev.*, **127**, 2709–2732, Corrigendum **128**, 27091573–2732.
- Schumacher, P. N., 2003: An example of forecasting mesoscale bands in an operational environment. Preprints, 10<sup>th</sup> Conf. on Mesoscale Processes, Portland, OR, Amer. Meteor. Soc., CD-ROM, P8.1.
- Wagner, K. R., 2006: Cool-season moderate precipitation events in the northeast United States. Master of Science Thesis, Department of Earth and Atmospheric Sciences, University at Albany / SUNY, Albany, NY, 134 pp.
- Wetzel, S. W., and J. E. Martin, 2001: An operational ingredients-based methodology for forecasting midlatitude winter season precipitation. *Wea. Forecasting.*, 16, 156-167.

Waldstreicher, J., 2001. The Importance of Snow Microphysics for Large Snowfalls.
 NOAA, National Weather Service, Eastern Region Headquarters, Scientific Services
 Division. [Available online at <a href="http://www.erh.noaa.gov/er/hq/ssd/snowmicro/">http://www.erh.noaa.gov/er/hq/ssd/snowmicro/</a>].

## FIGURE CAPTIONS

FIG. 1. Schematic cross section of the environment for a banded frontal zone. Saturation equivalent potential temperature (dashed), frontogenesis (ellipse), and transverse circulation (arrows) are shown, with dry air intrusion (light shading; an X depicts flow into the plane of the cross section) and areas exhibiting weak moist symmetric stability (WMSS; dark shading) overlaid. Expected location of precipitation band indicated by an asterisk (\*) along the *x* axis. [Adopted from Novak et al. (2006, Fig. 2)]

FIG.2. Correlations between observed maximum snowfall and *maximum/minimum magnitude* of several parameters derived from 0 h., 12 h., and 24 h. time-height diagrams. Correlations are Spearman coefficient of rank values.

FIG. 3. Same as Fig. 2, except that the correlations are between observed maximum snowfall and the *depth and persistence* of several parameters derived from 0, 12, and 24 h. forecasts from time-height diagrams. Correlations are Spearman coefficient of rank values.

FIG. 4. Histograms showing the relationship between snowfall and the existence of a) a \* Signature, and b) a deep, persistent \* Signature (from analysis data). Bars with grey shading indicate the number of events in each snowfall category associated with a \* Signature / deep persistent \* Signature. The bars shaded black indicate the number of events in each category not associated with a \* Signature / deep, persistent \* Signature.

FIG. 5. Scatter-plot diagrams of event total snowfall (cm, with inches in parentheses, x-

axis) vs. a) minimum omega within the dendrite zone ( $\mu$ b s<sup>-1</sup>, y-axis) and b) minimum omega ( $\mu$ b s<sup>-1</sup>, y-axis) in the entire column (without regard to thermal profile).

FIG. 6. (a) 12 UTC, December 5, 2003 NAM forecast time-height diagram at a point in east central New York: omega ( $\mu$ bs<sup>-1</sup>) contoured, EPVg\* (PVU, negative values shaded), and relative humidity (percent) contoured. (b) Same as (a), except from the 06 UTC, December 6, 2003 NAM. (c) 12 UTC, December 5, 2003 NAM forecast 600 hPa omega ( $\mu$ bs<sup>-1</sup>) contoured and 500 hPa EPVg\* (PVU, negative values shaded), valid at 06 UTC, December 6, 2003. (d) Same as (c), except from the 06 UTC, December 6, 2003 NAM.

FIG. 7. 00 UTC, April 16, 2007 NAM forecast vertical cross-sections, valid at (a) 06 UTC, April 16, 2007 and (b) 09 UTC, April 16, 2007. The cross-section axis is labeled from A' to A in Fig. 7d. Negative EPVg\* (PVU) is shaded and relative humidity (percent) is contoured. The approximate position of the snow band (based on radar imagery, Fig. 7d) is annotated. The ellipses depict the positions where EPVg\* (PVU) was most negative (with the magnitudes labeled). (c) 00 UTC, April 16, 2007 NAM forecast time-height diagram, (at the "X" shown on Fig. 7d), of omega ( $\mu$ bs<sup>-1</sup>, black contours, negative values dashed), EPVg\* (PVU, negative values shaded), and relative humidity (percent, gray contoured). (d) WSR-88D mosaic reflectivity over the northeastern United States at 0930 UTC, April 16, 2007 (only values greater than 20 dbz shown).

TABLE 1. The 25 events used in the study.

Date	Time	Maximum Snowfall (inches)	Time-Height Location
2/17/2003	1800 UTC	13	Broome County (NY)
3/30/2003	1200 UTC	8	Schuyler County (NY)
12/6/2003	1200 UTC	10	Chenango County (NY)
12/6/2003	1200 UTC	24	Columbia County * (NY)
12/15/2003	0000 UTC	18	Oneida County (NY)
1/28/2004	0000 UTC	10	Broome County (NY)
2/3/2004	2100 UTC	8	Broome County (NY)
3/16/2004	1200 UTC	12	Tioga County (NY)
12/27/2004	0000 UTC	6	Delaware County (NY)
1/8/2005	1800 UTC	5	Cortland County (NY)
1/19/2005	1800 UTC	7	Chenango County (NY)
1/23/2005	0600 UTC	14	Chenango County (NY)
1/23/2005	1500 UTC	34	Plymouth Co. (Mass) *
2/21/2005	0600 UTC	8	Oneida County (NY)
3/1/2005	0000 UTC	12	Pike County (PA)
3/2/2005	0000 UTC	8	Susquehanna County (PA)
3/24/2005	0000 UTC	9	Delaware County (NY)
12/9/2005	1200 UTC	13	Wayne County (PA)
12/16/2005	1200 UTC	10	Madison County (NY)
1/3/2006	0600 UTC	12	Sullivan County (NY)
1/15/2006	0000 UTC	4	Sullivan County (NY)
1/23/2006	1200 UTC	5	Sullivan County (NY)
2/12/2006	1200 UTC	26	Fairfield Co. (Conn) *
2/25/2006	1800 UTC	10	Oneida County (NY)
3/2/2006	1800 UTC	10	Schuyler County (NY)

\* Maximum snowfall recorded outside of the BGM CWA.

TABLE 2<sup>•</sup> Correlations between event maximum snowfall, and several parameters derived from 0-h forecasts *from conventional cross sections*, taken at the time of maximum snowfall intensity, or 3 hours prior to maximum snowfall intensity. Correlations are Spearman coefficient of rank values. Values denoted by asterisks are statistically significant at the 95 percent confidence level.

Parameter	Correlations with event maximum snowfall	
Minimum omega in the dendrite zone	0.63*	
Maximum depth of the dendrite zone	0.31	
Minimum omega	0.35*	
Maximum Fn convergence	0.54*	
Minimum EPVg* at t-3	0.58*	
Maximum depth of EPVg* < 0 PVU at t-3	0.48*	
Minimum EPVg* at t0	0.32	
Maximum depth of EPVg* < 0 PVU at t0	0.21	

TABLE 3. Correlations between event maximum snowfall, and event maximum magnitude of several parameters, *derived from time height diagrams*. Values denoted by asterisks are statistically significant at the 95 percent confidence level.

Parameter	Correlation with event maximum
	snowfall
Minimum Omega in the dendrite zone	0.32
Maximum Depth of the dendrite zone	0.21
Minimum Omega	0.18
Maximum Fn Convergence	0.37*
Minimum EPVg*	0.63*
Maximum depth of EPVg* < 0 PVU	0.37*

TABLE 4. Correlations between event maximum snowfall and depth and persistence of several parameters in the study, derived from time height diagrams. Parameters are listed from highest to lowest correlations. Values denoted by asterisks are statistically significant at the 95 percent confidence level.

Parameter	Correlation with event
	maximum snowfall
Depth and persistence of Omega $< -8 \ \mu b \ s^{-1}$ in the dendrite zone	0.70*
Depth and persistence of the * Signature	0.61*
Depth and persistence of Omega $< -8 \ \mu b \ s^{-1}$	0.59*
Depth and persistence of Negative EPVg*	0.56*
Depth and persistence of Fn convergence $> 5 \times 10^{-14}$ oC s <sup>2</sup> m <sup>-1</sup>	0.34*
Depth and persistence of the ** Signature	0.17

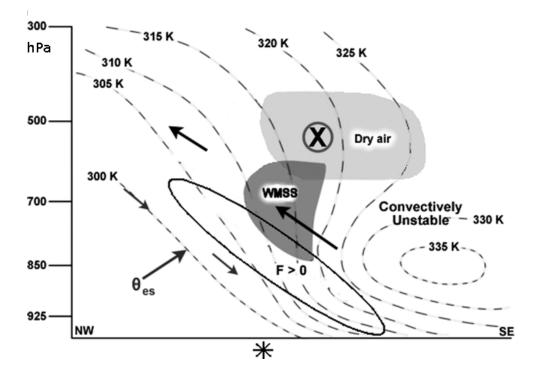


FIG. 1. Schematic cross section of the environment for a banded frontal zone. Saturation equivalent potential temperature (dashed), frontogenesis (ellipse), and transverse circulation (arrows) are shown, with dry air intrusion (light shading; an X depicts flow into the plane of the cross section) and areas exhibiting weak moist symmetric stability (WMSS; dark shading) overlaid. Expected location of precipitation band indicated by an asterisk (\*) along the *x* axis. [Adopted from Novak et al. (2006, Fig. 2)]

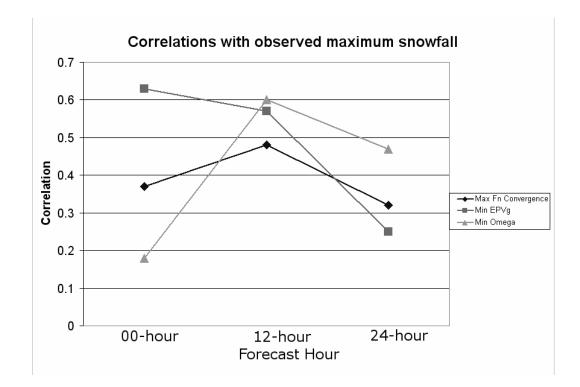


FIG.2. Correlations between observed maximum snowfall and *maximum/minimum magnitude* of several parameters derived from 0 h., 12 h., and 24 h. time-height diagrams. Correlations are Spearman coefficient of rank values.

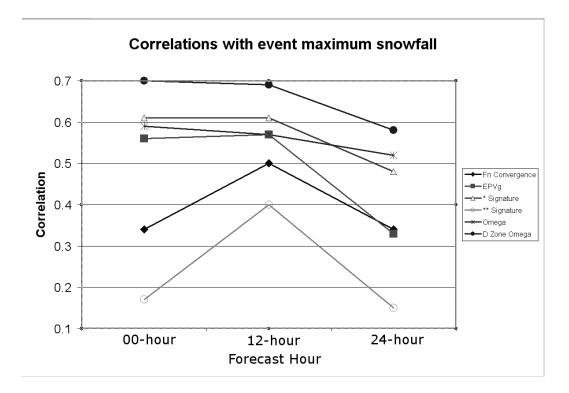


FIG. 3. Same as Fig. 2, except that the correlations are between observed snowfall and the *depth and persistence* of several parameters derived from 0, 12, and 24 h. forecasts from time-height diagrams. Correlations are Spearman coefficient of rank values.

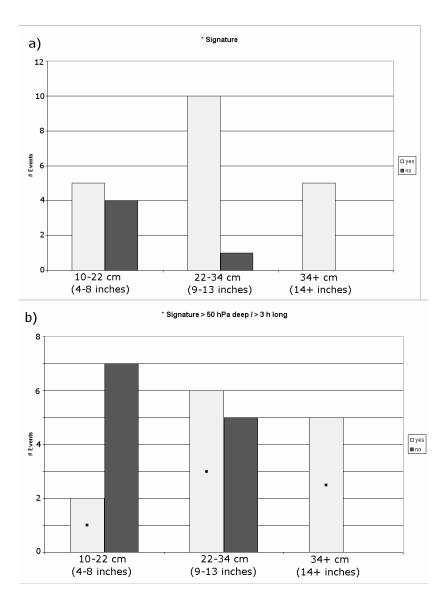


FIG. 4. Histograms showing the relationship between snowfall and the existence of a) a \* Signature, and b) a deep, persistent \* Signature (from analysis data). Bars with grey shading indicate the number of events in each snowfall category associated with a \* Signature / deep persistent \* Signature. The bars shaded black indicate the number of events in each category not associated with a \* Signature / deep, persistent \* Signature.

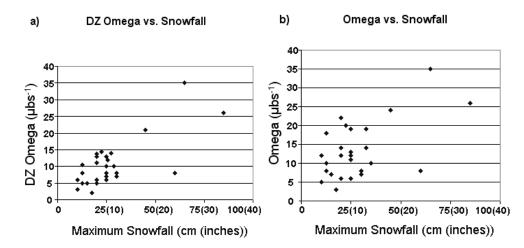


FIG. 5. Scatter-plot diagrams of event total snowfall (cm, inches in parentheses, x-axis) vs. a) minimum omega within the dendrite zone ( $\mu$ b s<sup>-1</sup>, y-axis) and b) minimum omega ( $\mu$ b s<sup>-1</sup>, y-axis) in the entire column (without regard to thermal profile).

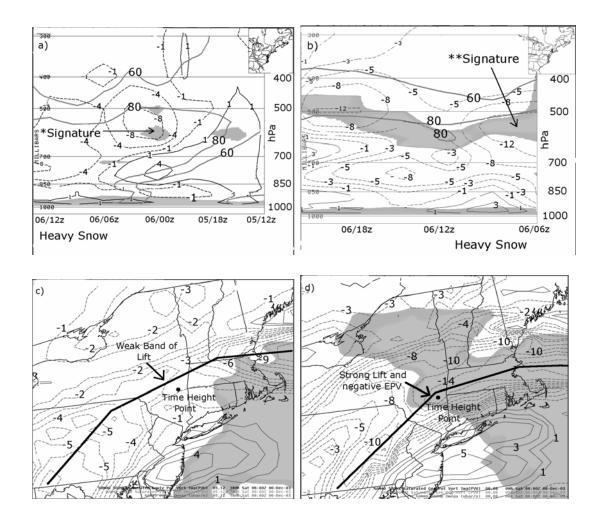


FIG. 6. (a) 12 UTC, December 5, 2003 NAM forecast time-height diagram at a point in east central New York (time increases from right to left): omega ( $\mu$ bs<sup>-1</sup>, thin contours), EPVg\* (PVU, negative values shaded), and relative humidity (60 and 80 percent values contoured, thick contours). The period of observed heaviest snow is annotated. (b) Same as (a), except from the 06 UTC, December 6, 2003 NAM. (c) 12 UTC, December 5, 2003 NAM forecast 600 hPa omega ( $\mu$ bs<sup>-1</sup>) contoured and 500 hPa EPVg\* (PVU, negative values shaded), valid at 06 UTC, December 6, 2003. Axis of minimum omega is annotated. (d) Same as (c), except from the 06 UTC, December 6, 2003 NAM.

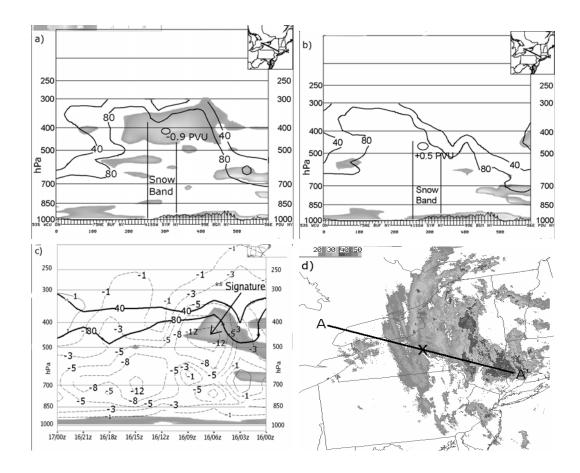


FIG.7. 00 UTC, April 16, 2007 NAM forecast vertical cross-sections, valid at (a) 06 UTC, April 16, 2007 and (b) 09 UTC, April 16, 2007. The cross-section axis is labeled from A' to A in Fig. 7d. Negative EPVg\* (PVU) is shaded and relative humidity (percent) is contoured. The approximate position of the snow band (based on radar imagery, Fig. 7d) is annotated. The ellipses depict the positions where EPVg\* (PVU) was most negative (with the magnitudes labeled). (c) 00 UTC, April 16, 2007 NAM forecast time-height diagram (at the "X" shown on Fig. 7d) of omega ( $\mu$ bs<sup>-1</sup>, black contours, negative values dashed), EPVg\* (PVU, negative values shaded), and relative humidity (percent, gray contoured). (d) WSR-88D mosaic reflectivity over the northeastern United States at 0930 UTC, April 16, 2007 (only values greater than 20 dbz shown).